1. Methodology

1.1 Introduction

To evaluate the performance of various support structures developed through topology optimization, a comparative study was conducted in which components fabricated via additive manufacturing were paired with distinct support structures. This investigation assumed that different structural configurations would exhibit varying thermal conductivity, thereby influencing the efficiency of heat dissipation from each material layer during the manufacturing process. Enhanced thermal conduction is anticipated to mitigate overall thermal deformation, as the manufactured component would experience reduced expansion due to a shorter duration of exposure to elevated temperatures.

This section will explain the full process employed to run the simulations and analyze the resultant data. An overview of the procedural framework is illustrated in Figure 1.1. The process starts from the creation of the CAD for the manufactured components, followed by the design and CAD creation of the corresponding support structures. The components and the support structures are then merged, and imported into the additive manufacturing software to simulate the results of manufacture. The results obtained from the manufacturing simulation are then subjected to analysis through graphical representations and statistical methods.

The subsequent sections explain in detail each stage of this process.

1.2 Component CAD

The components with simple geometries utilized in this study consist of a cube, three triangular components with different slopes, and three cylindrical components with dif-

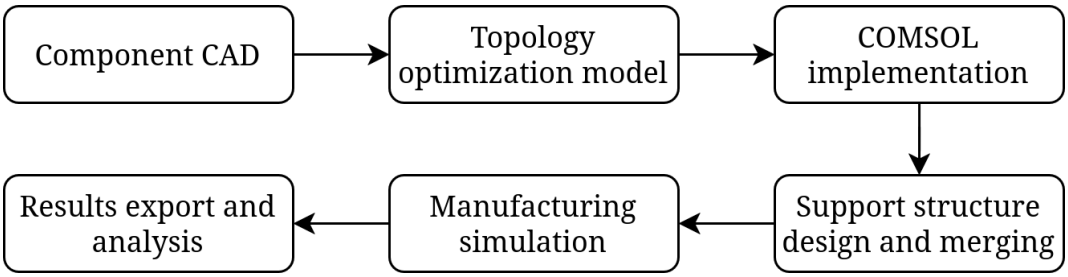

Figure 1.1: Process diagram.

ferent values of curvature. These shapes with these dimensions were chosen to ease the comparison of results between this study and the study of Peishu **chungpei-hsuStudyLatticeSupport2** All the CAD models used for the simple geometry study were created using FreeCAD **FreeCAD**, an open-source CAD software. The components were exported as .stp files, and then were merged with their corresponding support structures using the software nTop. The geometries used for this preliminary study are the following:

- A cube with side length of 30 mm, as shown in Figure 1.2.
- Three triangular components with varying slopes. All triangular components have a base of 30 x 30 mm^2, with slopes of 15°, 30°and 45 °. The measurements are shown in Figures 1.3a, 1.3b, and 1.3c.
- Three prisms with fillets of different. The radii used were 20 mm, 30 mm, and 40 mm. These rounded prisms also have a base of 30 x 30 cm^2. They are shown in Figures 1.4a, 1.4b, and 1.4c.

Apart from the parts above, a CAD model for a femoral component was also employed. The femoral component is one of the prosthetic components used in total knee arthroplasty, and is the piece that is directly connected to the patient's femur. This is shown in Figures 1.5 and 1.6.

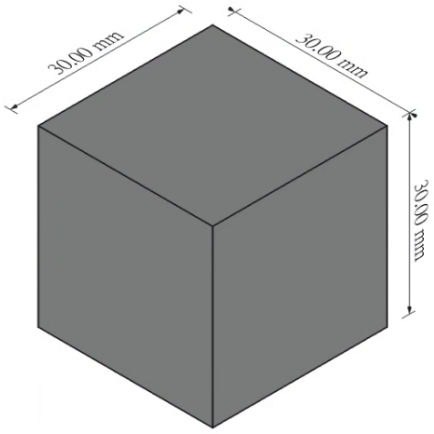

Figure 1.2: Dimensions of cube component.

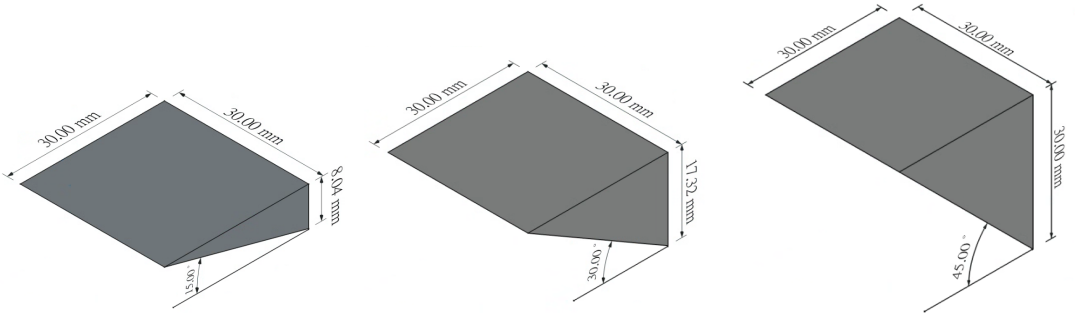

(a) 15°triangle. (b) 30°triangle. (c) 45°triangle.

Figure 1.3: Dimensions of triangular parts.

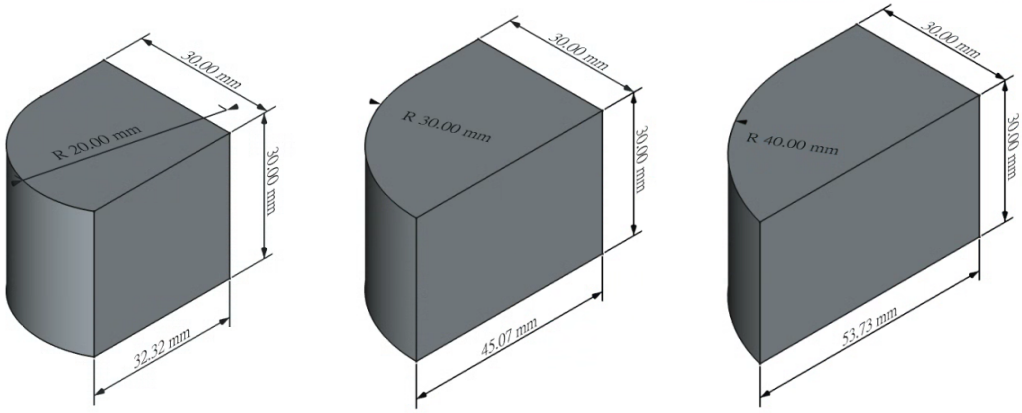

(a) Part with R20 mm fillet. (b) Part with R30 mm fillet. (c) Part with R40 mm fillet.

Figure 1.4: Dimensions of rounded parts.

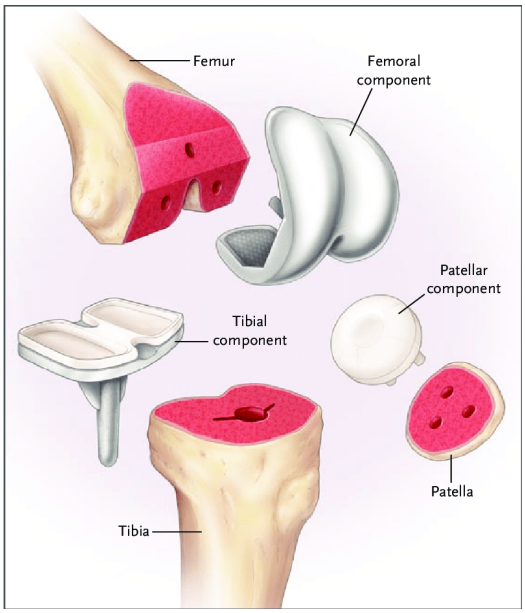

Figure 1.5: Components of total knee arthroplasty prosthesis. Taken from **leopoldMinimallyInvasiveTotal2009**.

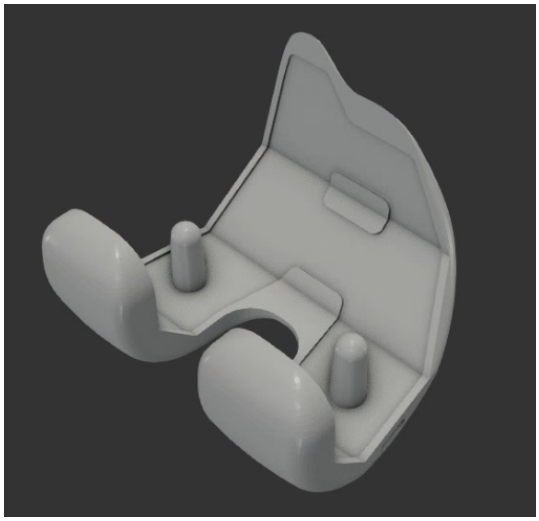

Figure 1.6: CAD model of femoral component.

1.3 Topology optimization model

The supporting structures of the components were created using the method of topology optimization. The design was implemented using the topology optimization module of COMSOL Multiphysics 6.2.

The steps for creating a valid topology optimization model are: determine the design volume, design the support structure using topology optimization, merge the support structure with the part, and carry out the FEM simulation for manufacture.

1.3.1 Design domain

The design domain consisted of the volume between the bottom face of each component and the xy plane, when the component is placed at a height of 30mm above the xy plane. For the simple geometry parts, as they have high symmetry, the design domain was just taken to be a 2D slice of the volume. The topology optimization problem was then solved for this volume, and the resulting topologies were extruded in the direction perpendicular to the design plane to cover the space underneath the part. For the femoral component, the topology optimization was directly solved in the 3D volume between the lower surface of the femoral component and the xy plane. Figures 1.7a and 1.7b show examples of design domains.

1.3.2 Objective functions

The objective of the problem is to maximize the thermal conduction of the support structure, while at the same time maximizing its stiffness. The thermal conductivity has been chosen as an objective since it is required to drive heat away from the part as fast as possible to reduce its thermal deformation. Thermal conduction is given by Fourier's law as:

$$\boldsymbol{Q} = -\kappa \nabla T \tag{1.1}$$

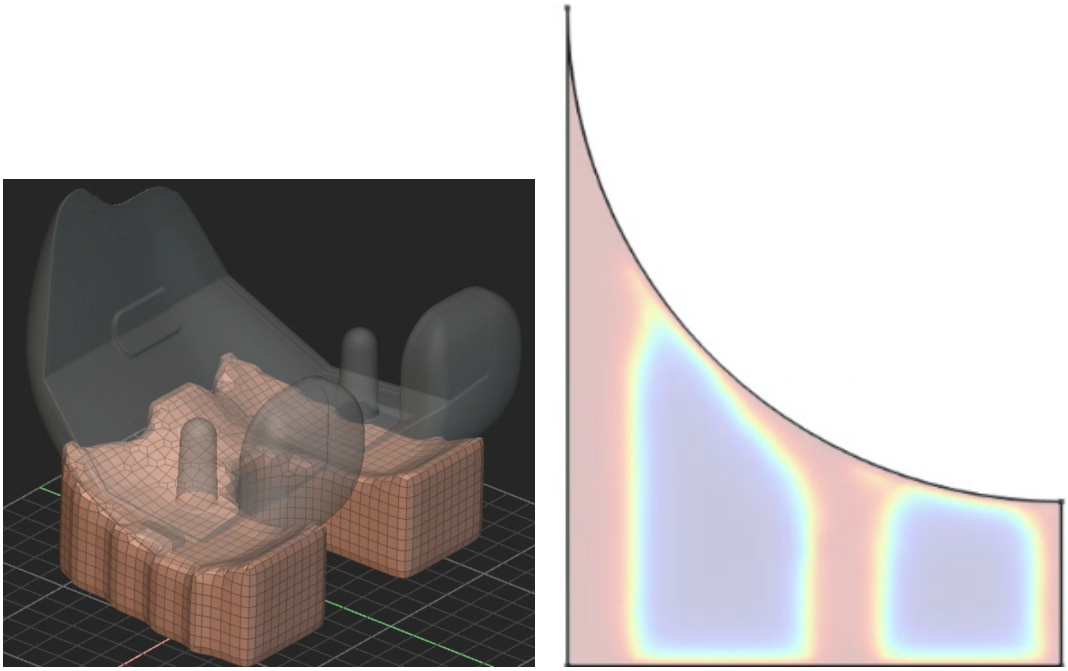

(a) Design domain for femoral component. (b) Design domain for rounded part.

Figure 1.7: Examples of design domains.

where $\boldsymbol{Q}$ is the heat conduction through the material, κ is the material's thermal conductivity and ∇T is the thermal gradient. For use in a finite element solver, the objective function c_t and Fourier's law can be written using matrix notation as:

$$\text{minimize} \quad c_t = \boldsymbol{Q}^{\boldsymbol{T}}\boldsymbol{T} \tag{1.2}$$

$$\boldsymbol{\kappa T} = \boldsymbol{Q}, \tag{1.3}$$

where $\boldsymbol{\kappa}$ is the global thermal conductivity matrix, $\boldsymbol{T}$ is the temperature vector, and $\boldsymbol{Q}$ is the thermal load, or heat flux, vector. Thermal compliance c_t can be thought of the thermal analogy to the stiffness of a structure. In structural problems, the objective is to maximize the stiffness, or minimize the compliance, as compliance is the inverse of stiffness. Similarly, in thermal problems, the objective is to maximize the thermal conductivity, or alternatively, minimize the thermal compliance, which can be though

of as the inverse of conductivity. Thermal compliance has extensively been used in other topology optimization problems such as **leeObjectiveFunctionTopology2021**, **yoonTopologicalDesignHeat2010**, and **brunsTopologyOptimizationConvectiondominated200**

At the same time, stiffness of the support structure should be be maximized to avoid considerable deformations that might affect the part geometry. The geometry resulting from the thermal optimization could result in thin, dendrite-like structures, which could buckle and collapse under the component's weight, causing the whole manufacturing process to fail. Assuming small deformations, we can express the displacement of the material by using Hooke's law, $\boldsymbol{F} = k\boldsymbol{U}$. For finite element analysis, the minimization of the compliance c of the structure and its mechanical behavior is obtained by minimizing the quantity $\boldsymbol{F^T U}$, by solving for $\boldsymbol{U}$ using a numerical method.

We can then combine the thermal and mechanical compliance to obtain the objective function for this topology optimization problem, with ω_1 and ω_2 the weight coefficients that encapsulate the relative importance of each objective: $\omega_1 \boldsymbol{Q^T T} + \omega_2 \boldsymbol{F^T U}$

1.3.3 Topology optimization equations

Having decided the governing equations and objective function for the system, the topology optimization model must be chosen. For this study, the SIMP approach with a hyperbolic tangent projection has been employed, utilizing a volume fraction restriction. Mathematically, the topology optimization problem is formulated as shown in equations **??** to **??** , where the density $\tilde{\rho}$ has been defined using the hyperbolic tangent projection function as defined in section **??**.

1.4 COMSOL implementation

1.4.1 Mesh

To run the topology optimization algorithm and obtain a solution, the design domain must be divided into finite element methods for computation. For the 2D design do-

mains of the simple geometry elements, free triangular meshes were utilized, using a predefined mesh element size of ”finer”. This resulted in about 2000-3000 elements for each of the design domains, depending on the geometry of the domain. These mesh parameters were chosen to produce fast results and to obtain a general idea of how the simulation parameters affected the solution of the topology optimization problem. An example of 2D mesh can be seen in Figure 1.8.

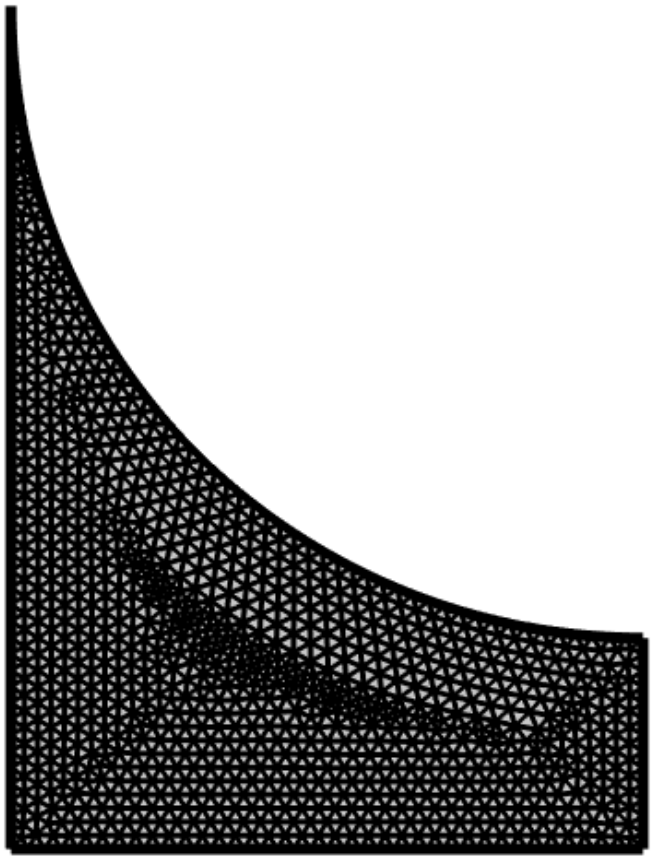

Figure 1.8: Mesh of the design domain for one of the rounded parts.

On the other hand, For the 3D design domain of the femoral component support structure, the mesh sizing parameters were chosen with more deliberation. The maximum and minimum element sizes of the mesh were determined based on the minimum element size achievable by the selective laser melting (SLM) machine utilized in this study, which is approximately 0.2 millimeters. However, employing a mesh with an ele-

ment size of 0.2 millimeters results in excessively fine meshes that significantly prolong computational solving times. Consequently, the maximum and minimum mesh sizes were adjusted to be 8 and 4 times the minimum feature size, resulting in values of approximately 1.6 millimeters and 0.8 millimeters, respectively. This resulted in meshes with approximately 164,000 elements. The resulting mesh can be seen in Figure 1.9.

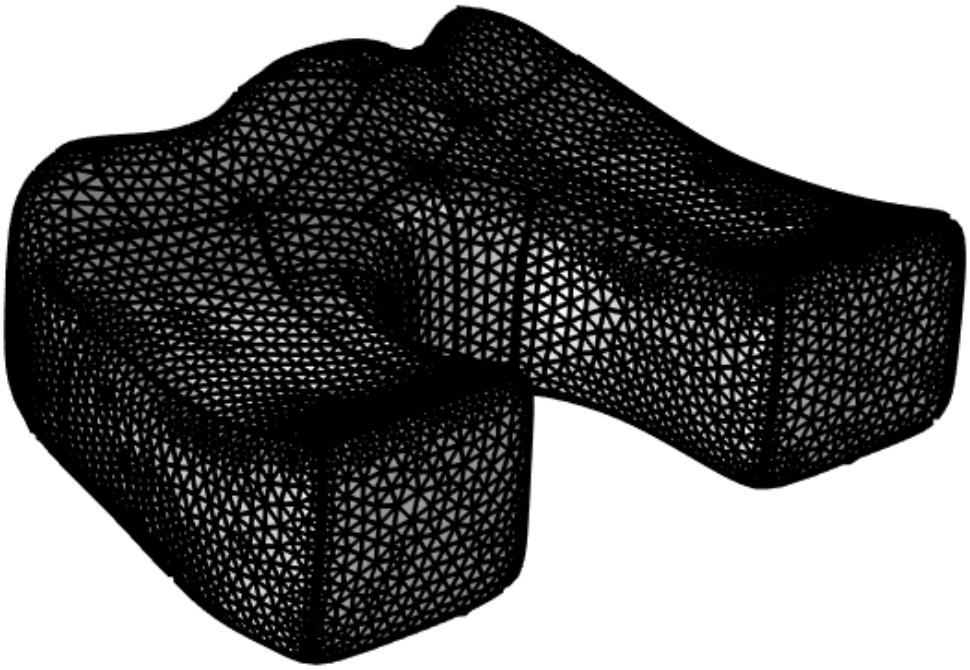

Figure 1.9: Mesh of the design domain for the support structure of the femoral component.

1.4.2 Physical parameters

For the topology optimization solution to be useful, realistic thermal and stress load should be used. The thermal load was based on the maximum wattage and efficiency of the laser achievable by the selective laser melting machine used in this work. The laser's

power is 200 W, with an efficiency of 25%. This value cannot be used for the thermal load, since the laser is only activated for a small amount of time. From the FEM software building process parameters, each layer is heated for approximately 154 ms. Therefore, with an effective power of 200 W x 0.25% = 50W, the total amount of energy added to the layer during the heating time is 50 W x 154 ms = 7.7 J. But each layer heating time occurs periodically, with a period of approximately 440 s. Therefore, the average power input to the system per cycle is calculated to be 0.0175 W. A graphical representation of this calculation is shown in Figure 1.10. The approximate area of the top surface of the support structure design domain is approximately 30 mm x 30 mm = 900 mm^2. Diving the power per cycle by this area yields a heat flux of about 19.4 W/mm^2, which was rounded up to 20.0 W/m^2. For the heat flux used in the femoral component calculation, the difference is in the area of the top surface of the design domain. This area is about 1690 mm^2, and thus the heat flux used for the support structure design in accounts to be about 10.37 W/m^2, which was rounded to 10 W/m^2.

The material used in all simulations was 316L stainless steel. This material is often used for medical implants due to its superior mechanical, fatigue, wear and corrosion properties **davisComprehensiveReviewMetallic2022**. The mechanical and thermal properties of 316L steel relevant to this study are shown in Table 1.1.

Table 1.1: Physical properties of 316L steel.

Density	8.0 g / cm^3
Thermal conductivity	15 W / (m·K)
Heat capacity	500 J / (kg·K)
Young's Modulus	200 GPa

It should be noted that the physical properties of stainless steel shown above are average properties at 20°C. These are subject to change during the building process, as the material is repeatedly heated above its melting point and cooled down, but for the purpose of simplifying the simulation process, these constant values were employed for

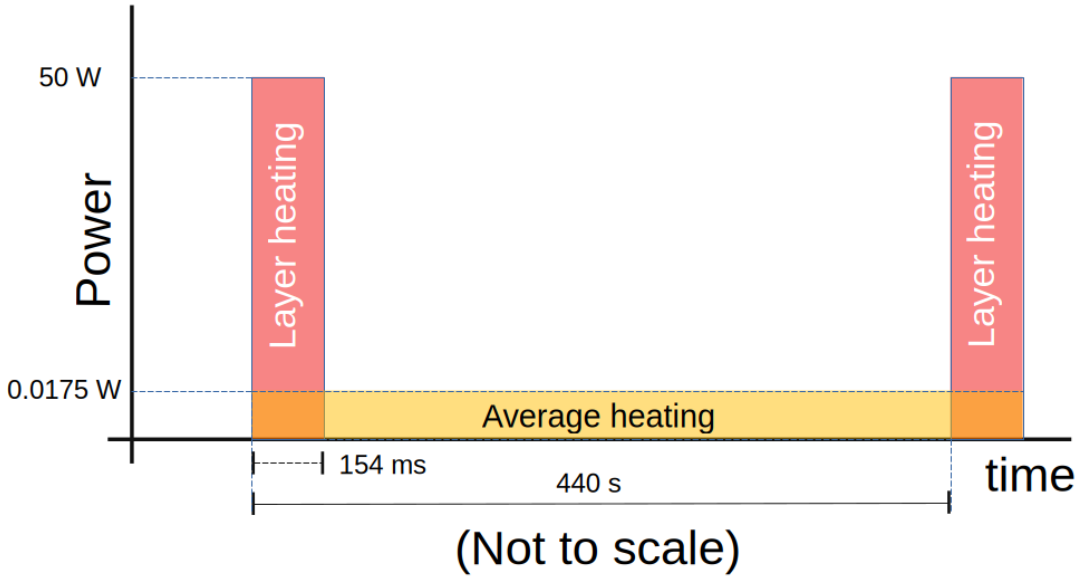

Figure 1.10: Layer heating cycle.

the topology optimization problem.

For the calculation of compliance, the structural load used was the stress on the top surface of the design domain caused by the weight of the component above it. This stress was calculated by diving the component's weight by the area of the top surface. The weight was determined using the density of 316L steel, which is approximately 7.93 g/cm^3. For example, the volume of the femoral component was calculated to be about 32800 mm^3, and therefore the mass of the femoral component amounts to approximately 0.263 kg. From this, the weight can be calculated by multiplying by the gravitational constant g, and the stress is obtained by dividing this weight by the top area of the design domain. The calculation for this example ends up being (0.263 kg)g /1690 mm^2 = 1560 N/m^2, where g is taken to be 9.81 m/s^2.

1.4.3 Parametric study

The topology optimization problem was solved using COMSOL Multiphysics 6.2 software. COMSOL allows the creation of parametric studies that allow to run a simulation with a list of parameters to be varied, in order to study the influence of different values

on the solution of a system. For this study, the values of volume fraction **??**, objective function weights **??**, and hyperbolic tangent angle (used in **??**) were chosen as the parameters to be varied.

Volume fraction is defined as the maximum amount of volume that the topology can cover within the design domain. This criteria is chosen because we seek to use less material for the supporting structure, as long as we can maintain the total deformation of the manufacturing component beneath a threshold. For the simple geometries 50% and 75% of volume fraction were considered. For the femoral component study, volume fractions of 25%, 33%, 40%, 50% and 75% were considered.

The hyperbolic tangent angle projection (**??**) was also used as a parameter. The hyperbolic tangent was varied from a value of 0.001°to 8°, in steps in 2°. The variation was stopped at 8°since it was noticed that for $\theta \geq 8°$there would be no discernible differences between results.

Finally, the objective functions weights were also varied for the design of topologies for the simple geometry parts. The pairings of weight used were (0.2, 0.8), (0.5 , 0.5), and (0.2, 0.8), where the first weight in each pair corresponds to the weight of the thermal compliance objective and the second corresponds to the weight of the mechanical compliance objective. All of these parameters are summarized in Table 1.2.

1.4.4 Boundary conditions

It is possible to change the material boundary conditions in COMSOL when solving the topology optimization problem. As an extra study parameter, the material boundary condition of several edges of the design domain were also varied for this study. For the 2D design domains, different topologies were obtained by having either a prescribed material or void boundary in the side elements of the design domain. For the femoral component, there was no variation in the density of the design domain boundary. Figures 1.12a and 1.12bshows the boundary conditions used in the problem.

The heat transfer and solid mechanics boundary conditions must also be specified.

Table 1.2: Variation of parameters.

Parameter	Values	
Volume fraction	Simple geometry	0.50, 0.75
	Femoral component	0.25, 0.33, 0.40, 0.50, 0.75
Hyperbolic tangent angle	Simple geometry	0.001°, 2°, 4°, 8°
	Femoral component	0.001°, 2°, 4°, 8°
Boundary conditions	All	void (no material at boundaries)
		material (material at boundaries)
Objective weights	Simple geometry	(0.2, 0.8), (0.5, 0.5), (0.8, 0.2)
	Femoral component	(1.0, 0.0)

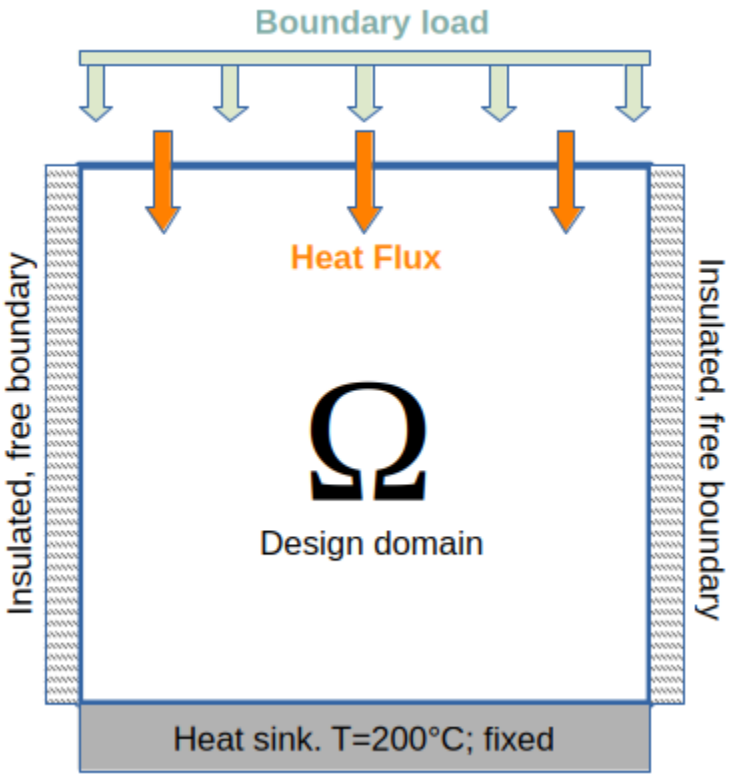

Figure 1.11: Boundary condition examples for design domain of cube component.

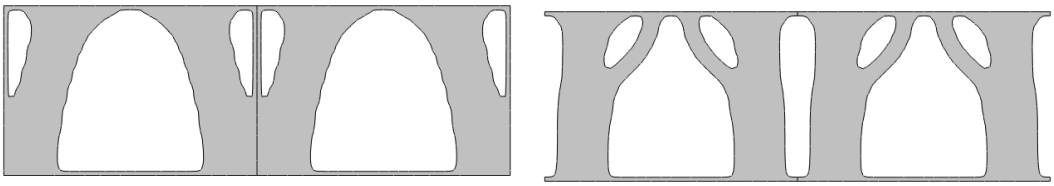

(a) Topology with solid material density. (b) Topology with void material density.

Figure 1.12: Variation in topology due to material prescribed density at the side boundary of design domain.

The heat transfer problem boundary conditions consisted of a heat flux through the upper surface of 20 W / (m^2·K) and 10 W / (m^2·K) for the simple geometry parts and femoral component respectively. The inferior surface was set at a constant temperature of 200°K, and the sides were kept insulated. The structural loads consisted of the weight of the component above it. Figure 1.11 shows a graphical representation of the boundary conditions used.

1.4.5 COMSOL implementation final details

Once all the physical and material parameters, the topology optimization model and parameters, boundary conditions, and parametric study have been set up, the solver will have all the information needed to obtain a solution. For this project, the solver algorithm utilized the method of moving asymptotes (MMA) **svanbergMethodMovingAsymptotes1987**, with a maximum iteration number of 50. The optimality tolerance was also set to COMSOL's default value of 0.001. Lastly, the penalty factor for the SIMP method was set to p=3.

1.5 Support structure design and merging with part

After COMSOL was used to generate the possible topologies for the support structure, the topology was exported to image files, in the case of the 2D problem, and to an .stl file, in the case of the 3D structure. These were then converted to 3D .stp file with the aid of FreeCAD. nTop Software **NTop** was then used to merge the resulting support

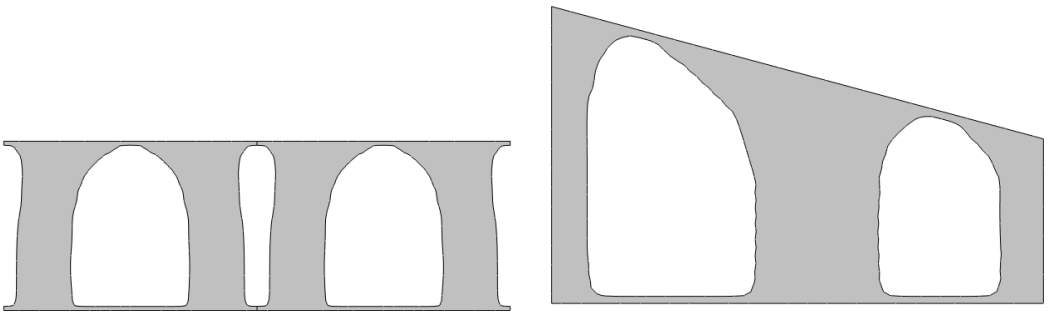

Figure 1.13: Examples of resulting topologies from COMSOL.

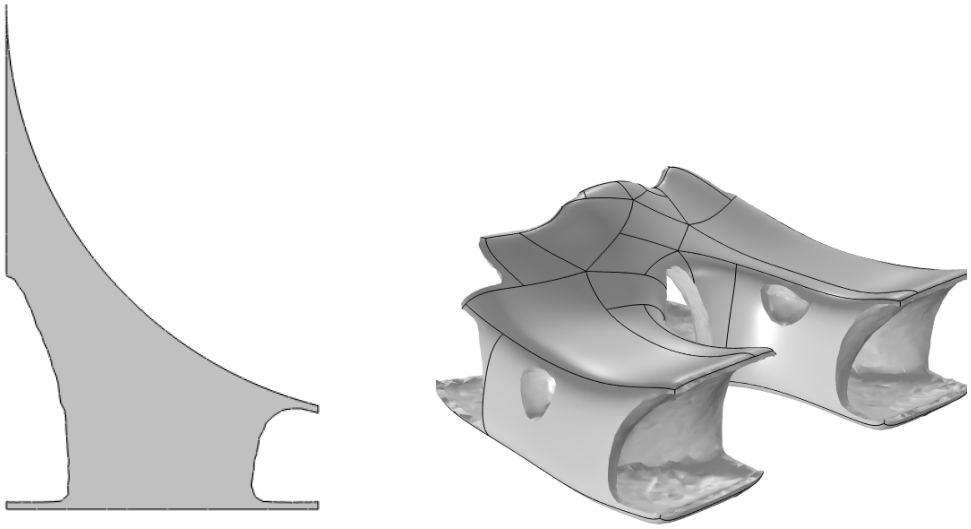

Figure 1.14: More examples.

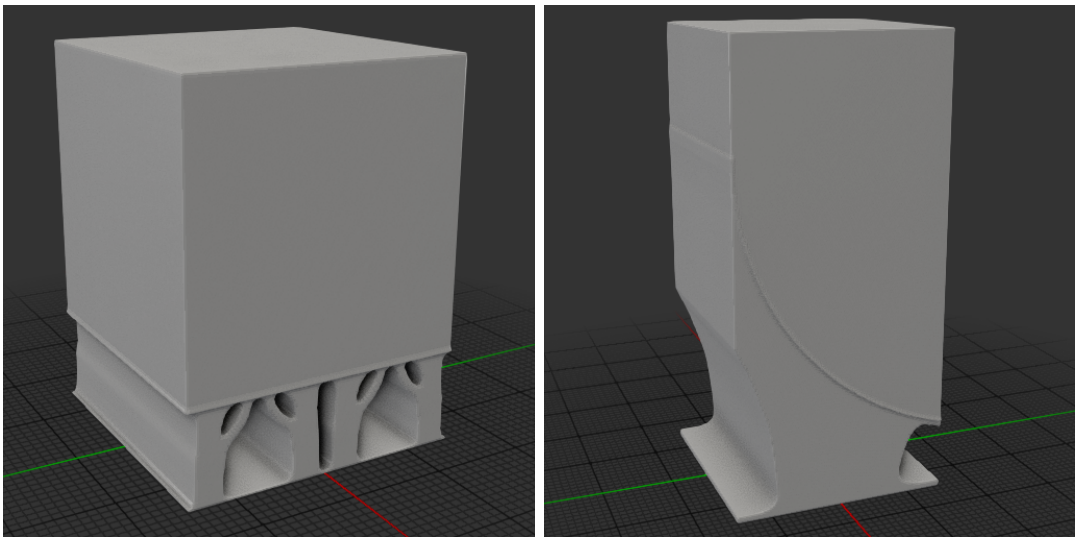

Figure 1.15: Melds of support structures for cube and rounded part.

structure with the manufactured components. Once the support structure and the part were joined, they were exported as .stl files to be used in the SLM finite element simulation.

Once the CAD file of the component and the support structure has been built, it is necessary to merge them together and import them into Simufact to undergo simulation of the manufacturing process. The software used for blending the component and its support structure is nTop version 5.17.2. nTop's interface makes it very easy to merge the part, and also allows to blend the support structure and the component, which effectively creates a fillet between the nodes of both components to allow for a smooth transition between bodies. Of course, blending the component and the support structure in this manner would not give any benefit in a real manufacturing process, as the structure and the component would not be able to be separated easily. Nevertheless, this blend radius is beneficial for the simulation since it was observed that a direct union and import of the support structure + component in Simufact resulted in having very small gaps between the two pieces, resulting in a non manifold geometry that would cause the finite element model to have gaps between some of its nodes.

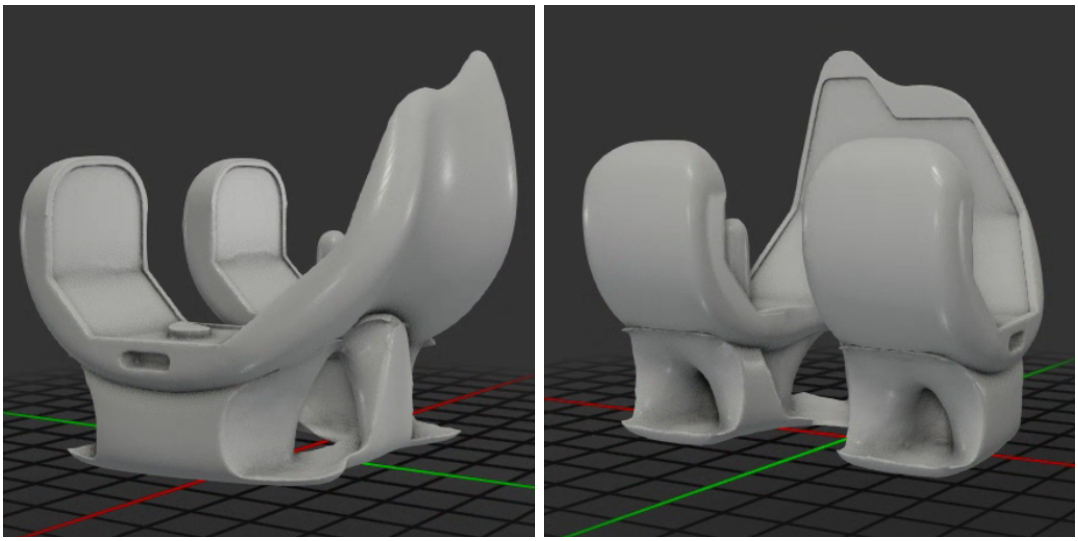

Figure 1.16: Meld of supporting structure for femoral component.

1.6 Simulation of manufacturing process

The software utilized to simulate the manufacturing process is Simufact Additive version 2023.2. Simufact Additive is capable of simulation building process of additive manufacturing components, and coupling thermal and stress physics to predict the temperature values of the component throughout the building process and the total stresses, strains and deformations resulting from the manufacturing process.

1.6.1 Process properties

After the component and the support structures were merged, they were imported into Simufact. It is during this step that all the factors related to the simulation are set, which include the machine properties, material properties, and build parameters.

The first parameter to be chosen is the process properties, which determines the physics that Simufact takes into consideration to run the simulation. Simufact provides three different types of processes: mechanical, thermal, and thermomechanical. As stated in the Simufact manual **hexagonabProcessPropertiesInfosheet**, mechanical provides a fast mechanical analysis that only uses inherent strains as the main input.

This type of analysis does not take into consideration the temperature fields during the building process. The thermal process on the other hand only considers the thermal behaviour of the components, and the temperature field of the support structures, components and base can be analyzed. The thermomechanical process couples the stress and thermal analyses, and allows for the prediction of temperature, distortions and stresses of the part. This latter thermomechanical process is the process utilized throughout this study.

1.6.2 Machine and build parameters

After choosing the process property, the machine parameters must be specified. This includes the machine build plate geometry and the laser parameters. The machine build plate chosen was a circular plate with an 80 mm radius. The build space dimensions consists of a space of 160 mm in all three x-y-z directions. As for the laser parameters, the simulations were carried out with one laser with a maximum laser power of 500 W and a maximum laser speed of 2000 mm / s, an efficiency of 25%, and a beam width of 25 mm. These machine parameters were modeled after an AMP-160 SLM machine, manufactured by TongTai Machine & Tool Company, Taiwan, that has been used in similar studies **chungpei-hsuStudyLatticeSupport2024**, **chungEvaluationPredictionThermal2024a**.

The building parameters for the process need also to be set. These include material layer parameters and any thermal parameters and temperature specifications for the build environment and base plate. The powder layer thickness was chosen to be 0.03 mm, with a recoater time of 10 s. The powder initial temperature was set to 25°C, with an initial base temperature of 200°C. Preheating is important in SLM since it can influence the quality of the microstructure of the component. It has been suggested that a temperature of 200°C exhibits higher cooling rates and smaller grain sizes of the microstructure **chowdhuryEffectsPreheatingThermal2024**.

All of the above parameters plus more are summarized in Tables 1.3, 1.4, 1.5, and

Table 1.3: Laser parameters

laser power	200W
laser speed	1000 mm/s
efficiency	25%
beam width	100 μm
layer thickness	30 μm
recoater time	10 s

Table 1.4: Scanner parameters

scan width	20 mm
scan overlap	0 mm
hatch distance	0.07 mm
pause time	0 s

1.6.

1.6.3 Convergence analysis

To ensure that FEM results were not dependent on the voxel size of the voxel mesh, a convergence analysis was first performed on one of the simple geometries. For this analysis, the results of three projects were compared. The details of the projects are shown in Table 1.7. The convergence test proved highly successful, as there is very little difference in the results of the FEM simulations between the different voxel sizes

Table 1.5: Thermal parameters

powder temperature	25°C
chamber temperature	50°C
base plate temperature	200°C

Table 1.6: Advanced thermal parameters

Part / Support emissivity	0.85
Part / Support heat transfer coefficient	12.0 W/(m^2·K)
Base plate emissivity	0.6
Base plate heat transfer coefficient	20 W/(m^2·K)
Base plate contact heat transfer coefficient	100 W/(m^2·K)

of each project. The results of the convergence test are shown in Figure 1.17. The graphs shows the average and max node deformation of the part's surface, as the voxel size is varied from 1 mm to 0.5 mm. We can see that the variability of surface results due to the voxel size is at most 0.01 mm. In subsequent analyses, the difference between average node displacements of parts with different support structures would be of an order of magnitude bigger ($>$ 0.1 mm), and thus we can discard the possibility that differences in results are caused or are dependent on the voxel mesh size.

Table 1.7: Parameters of support structures and geometries for convergence study.

Part	**Volfrac**	**tanh(θ)**	**Objective weights**	**Side density**
Cube 1	50%	0°	w1=w2=0.5	Solid
Cube 2	75%	4°	w1=w2=0.5	Void
Triangle 15°	50%	0°	w1=w2=0.5	Solid

1.6.4 Voxelization and numerical parameters

All of the simulations run on Simufact used voxel meshes with sizes ranging from 0.8 mm to 1.5 mm, depending on the complexity of the geometry of the part. The voxelization of the components was performed with Simufact's default voxelization engine. The voxel meshes of the components were uniform in size, while the base plate voxel mesh used adaptive meshing, with 2 levels of coarsening. The solver used for all simulations

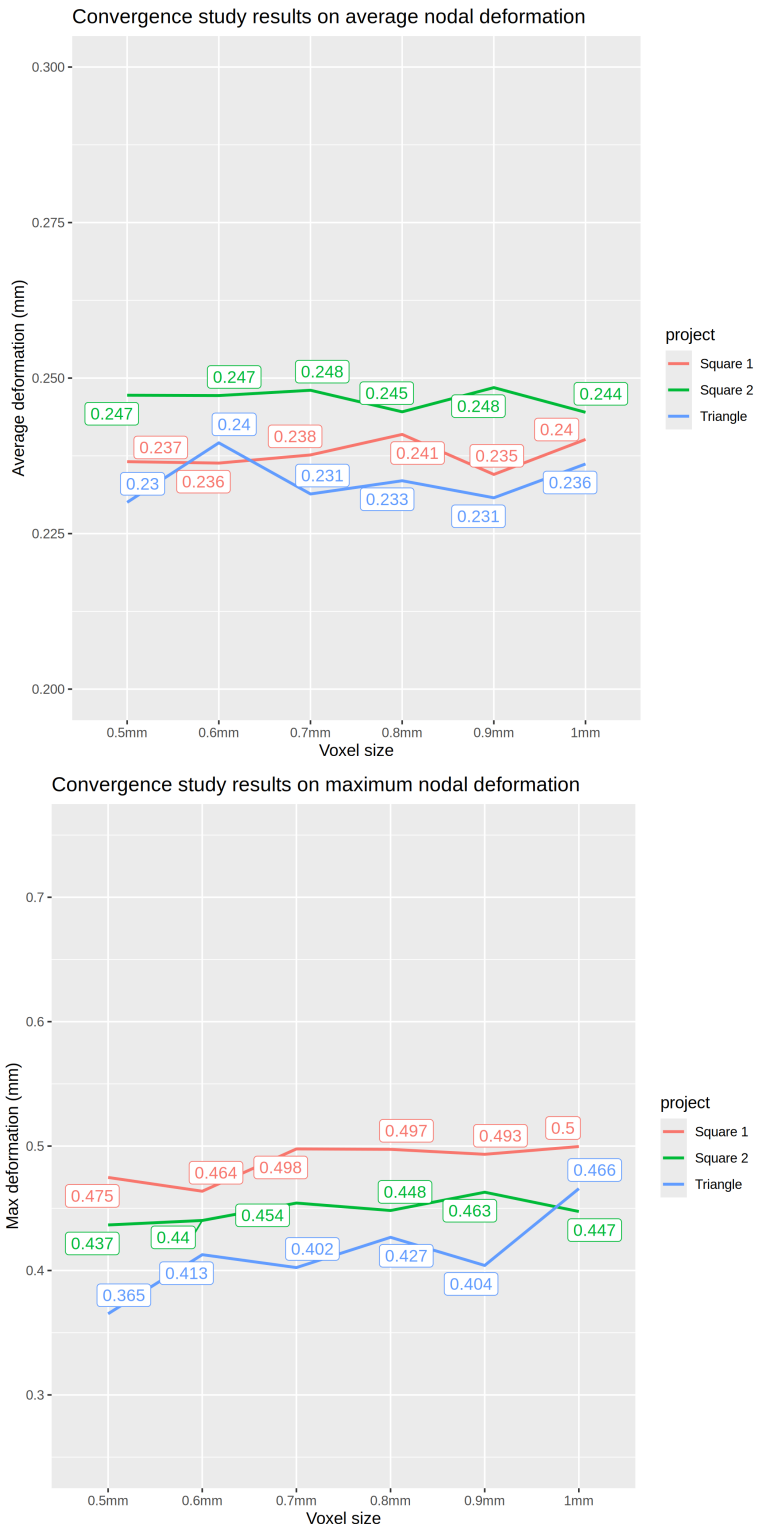

Figure 1.17: Results of convergence test on selected parts.

was the Multifrontal Massively Parallel Sparse (MUMPS for short) Direct Solver, with 14 time steps for each voxel layer.

1.7 Results and analysis

After the simulation was run, the node displacement and stress data of last time increment was exported to a .csv file using a Python script. The .csv file was then read and parsed using R, and the data was used to obtain statistical values and graphs. The results are summarized in the next chapter.